Relation between baryon number fluctuations and experimentally observed proton number fluctuations in relativistic heavy ion collisions

Masakiyo Kitazawa* and Masayuki Asakawa†
Department of Physics, Osaka University, Toyonaka, Osaka 560-0043, Japan
(Received 15 May 2012; published 7 August 2012)

We explore the relation between proton and nucleon number fluctuations in the final state in relativistic heavy ion collisions. It is shown that the correlations between the isospins of nucleons in the final state are almost negligible over a wide range of collision energy. This leads to a factorization of the distribution function of the proton, the neutron, and their antiparticles in the final state with binomial distribution functions. Using the factorization, we derive formulas to determine nucleon number cumulants, which are not direct experimental observables, from proton number fluctuations, which are experimentally observable in event-by-event analyses. With a simple treatment for strange baryons, the nucleon number cumulants are further promoted to the baryon number ones. Experimental determination of the baryon number cumulants makes it possible to compare various theoretical studies directly with experiments. The effects of nonzero isospin density on this formula are addressed quantitatively. It is shown that the effects are well suppressed over a wide energy range.

DOI: 10.1103/PhysRevC.86.024904 PACS number(s): 12.38.Mh, 25.75.Nq, 24.60.Ky

I. INTRODUCTION

Now that the observation of quark-gluon matter in relativistic heavy ion collisions has been established for small baryon chemical potential ($\mu_{\rm B}$) [1], a challenging experimental subject following this achievement is to reveal the global structure of the QCD phase diagram on the temperature (T) and μ_B plane. In particular, finding the QCD critical point(s), whose existence is predicted by various theoretical studies [2,3], is one of the most intriguing problems. Since the value of $\mu_{\rm B}$ of the hot medium created by heavy ion collisions can be controlled by varying the collision energy per nucleon pair, $\sqrt{s_{\rm NN}}$, the $\mu_{\rm B}$ dependences of the nature of the QCD phase transition should be observed as the $\sqrt{s_{\rm NN}}$ dependence of observables. An experimental project to explore such signals in the energy range $10 \lesssim \sqrt{s_{\rm NN}} \lesssim 200$ GeV, called the energy scan program, is now ongoing at the Relativistic Heavy Ion Collider (RHIC) [4,5]. Experimental data which will be obtained in future experimental facilities designed for lower-beam-energy collisions will also provide important information on this subject [6].

Observables which are suitable to analyze bulk properties of the matter around the phase boundary of QCD in heavy ion collisions are fluctuations [7]. Experimentally, fluctuations are measured through event-by-event analyses [4]. Theoretically, it is predicted that some of them, including higher order cumulants, are sensitive to critical behavior near the QCD critical point [8–12] and/or locations on the phase diagram, especially on which side the system is, the hadronic side or the quark-gluon side [13–19].

Among the fluctuation observables, those of conserved charges are believed to possess desirable properties to probe the phase structure in relativistic heavy ion collisions. One of the advantages of using conserved charges is that the characteristic times for the variation of their local densities are longer than those for nonconserved ones, because the variation of the local densities of conserved charges are achieved only through diffusion [13,14]. The fluctuations of the former thus can better reflect fluctuations generated in earlier stages of fireballs, when the rapidity coverage is taken sufficiently large. From a theoretical point of view, an important property of conserved charges is that one can define the operator of a conserved charge, Q, as a Noether current. Moreover, their higher order cumulants, $\langle \delta Q^n \rangle_c$, are directly related to the grand canonical partition function $Z(\mu) = {\rm Tr} e^{-\beta(H-\mu Q)}$ as

$$\langle \delta Q^n \rangle_c = T^n \frac{\partial^n \log Z(\mu)}{\partial \mu^n}, \tag{1}$$

with H and μ being the Hamiltonian and the chemical potential associated with Q, respectively. These properties make the analysis of cumulants of conserved charges well defined and feasible in a given theoretical framework. For example, they can be measured in lattice QCD Monte Carlo simulations [20–24]. Equation (1) also provides an intuitive interpretation for the behavior of higher order cumulants of conserved charges. For instance, the third-order cumulant of the net baryon number, $N_{\rm B}^{\rm (net)}$, satisfies $\langle (\delta N_{\rm B}^{\rm (net)})^3 \rangle_c = T \partial \langle (\delta N_{\rm B}^{\rm (net)})^2 \rangle_c / \partial \mu_{\rm B}$. This formula means that $\langle (\delta N_{\rm B}^{\rm (net)})^3 \rangle_c$ changes its sign around the phase boundary on the T-$\mu_{\rm B}$ plane where the baryon number susceptibility $\langle (\delta N_{\rm B}^{\rm (net)})^2 \rangle_c$ has a peak structure [17]. The change of the sign of observables like this will serve as a clear experimental signal [17–19].

QCD has several conserved charges, such as baryon and electric charge numbers and energy. Among these conserved charges, theoretical studies suggest that the cumulants of the baryon number have the most sensitive dependences on the phase transitions and phases of QCD. In order to see this feature, let us compare the baryon number cumulants with the electric charge ones. First, the baryon number fluctuations show the critical fluctuations associated with the QCD critical point more clearly. Although the baryon and electric charge

*kitazawa@phys.sci.osaka-u.ac.jp
†yuki@phys.sci.osaka-u.ac.jp

number fluctuations diverge with the same critical exponent around the critical point, it should be remembered that this does not mean similar clarity of signals for the critical enhancement in experimental studies. Fluctuations near the critical point are generally separated into singular and regular parts, and only the former diverges with the critical exponent. The singular part of the electric charge fluctuations is relatively suppressed compared to the baryon number ones, because the former ones contain isospin number fluctuations, which are regular near the critical point [9]. The additional regular contribution makes the experimental confirmation of the enhancement of the singular part difficult, and this tendency is more pronounced in higher order cumulants [17]. While it is known that proton number fluctuations in the final state also reflect the critical enhancement near the critical point [9], as we will show later the baryon number fluctuations are superior to this observable, too, in the same sense. Second, the ratios of baryon number cumulants [16] behave more sensitively to the difference of phases, i.e., hadrons or quarks and gluons. This is because the ratios depend on the magnitude of charges carried by the quasiparticles composing the state [13,14,16], while the charge difference between hadrons and quarks is more prominent in the baryon number.

Experimentally, however, the baryon number fluctuations are not directly observable, because chargeless baryons, such as neutrons, cannot be detected by most detectors. Proton number fluctuations can be measured [4,5], and recently its cumulants have been compared with theoretical predictions for baryon number cumulants. Indeed, in a free hadron gas in equilibrium the baryon number cumulants are approximately twice the proton number ones, because the baryon number cumulants in a free gas are simply given by the sum of those for all baryons, and the baryon number is dominated by proton and neutron numbers in the hadronic medium relevant to relativistic heavy ion collisions. In general, however, these cumulants behave differently. In fact, we will see later that the nonthermal effects which exist in baryon number cumulants are strongly suppressed in the proton number ones.

In heavy ion collisions, because of the dynamical evolution the medium at kinetic freeze-out is not completely in thermal equilibrium. The original ideas to exploit fluctuation observables of conserved charges as probes of primordial properties of fireballs [13,14] dealt with this nonthermal effect encoded in the final state as a hysteresis of the time evolution. To observe such effects, it is highly desirable to measure baryon number cumulants, which are expected to retain more effects of the phase transition and the singularity around the critical point. The experimental determination of baryon number cumulants also makes the comparison between experimental and theoretical studies more robust, since many theoretical works including lattice QCD simulations are concerned with the baryon number cumulants, not the proton number ones.

In Ref. [25], the authors of the present paper have argued that, whereas the baryon number cumulants are not the direct experimental observables as discussed above, they can be determined in experiments by only using the experimentally measured proton number fluctuations for $\sqrt{s_{\rm NN}} \gtrsim 10$ GeV. The key idea is that isospins of nucleons in the final state are almost completely randomized and uncorrelated, because of reactions of nucleons with thermal pions in the hadronic stage, as will be elucidated in Sec. II. This leads to the conclusion that, when $N_{\rm N}$ nucleons exist in a phase space of the final state, the probability that N_p nucleons among them are protons follows the binomial distribution. More generally, the probability distribution that N_p protons, N_n neutrons, $N_{\bar{p}}$ antiprotons, and $N_{\bar{n}}$ antineutrons are found in the final state in a phase space is factorized as

$$\mathcal{P}_{\rm N}(N_p,N_n,N_{\bar{p}},N_{\bar{n}}) = \mathcal{F}(N_{\rm N},N_{\bar{\rm N}})B_r(N_p;N_{\rm N})B_{\bar{r}}(N_{\bar{p}};N_{\bar{\rm N}}), \tag{2}$$

where the nucleon and antinucleon numbers are $N_{\rm N} = N_p + N_n$ and $N_{\bar{\rm N}} = N_{\bar{p}} + N_{\bar{n}}$, respectively, and

$$B_r(k;n) = \frac{n!}{k!(n-k)!} r^k (1-r)^{n-k} \tag{3}$$

is the binomial distribution function with probabilities $r = \langle N_p\rangle/\langle N_{\rm N}\rangle$ and $\bar{r} = \langle N_{\bar{p}}\rangle/\langle N_{\bar{\rm N}}\rangle$. The function $\mathcal{F}(N_{\rm N},N_{\bar{\rm N}})$ describes the distribution of nucleons and antinucleons and the correlation between them in the final state, which are determined by the dynamical history of fireballs. Using the factorization Eq. (2), one can obtain formulas to represent the (anti)nucleon number cumulants by the (anti)proton number ones, and vice versa; whereas the neutron number is not determined by experiments, this missing information can be reconstructed with the knowledge for the distribution function, Eq. (2). The (anti)nucleon number in Eq. (2) can further be promoted to the (anti)baryon number in practical analyses with a simple treatment for strange baryons to a good approximation. These formulas enable one to determine the baryon number cumulants solely with the experimentally measured proton number fluctuations, and, as a result, to obtain insights into the present experimental results on the proton number cumulants.

The main purpose of the present paper is to elaborate upon the discussion in Ref. [25] with some extensions. In Ref. [25] the formulas are derived only for an isospin-symmetric medium. In the present study we extend them to incorporate cases with nonzero isospin densities. With the extended relations, it is shown that the effect of nonzero isospin density is well suppressed for $\sqrt{s_{\rm NN}} \gtrsim 10$ GeV. The procedures of the manipulations and discussions omitted in Ref. [25] are also addressed in detail.

In the next section, we show that the factorization given by Eq. (2) is well applied to the nucleon and baryon distribution functions in the final state in heavy ion collisions. We then derive formulas to relate baryon and proton number cumulants in Sec. III. In Sec. IV, we discuss the recent experimental results at STAR [4,5] using the results in Sec. III, and possible extensions of our results. The final section is devoted to a short summary.

Throughout this paper, we use N_X to represent the number of particles X leaving the system after each collision event, where $X = p$, n, N, and B represent proton, neutron, nucleon, and baryon, respectively, and their antiparticles, $\bar{p}$, $\bar{n}$, $\bar{\rm N}$, and $\bar{\rm B}$. The net and total numbers are defined as $N_X^{\rm (net)} = N_X - N_{\bar{X}}$ and $N_X^{\rm (tot)} = N_X + N_{\bar{X}}$, respectively.

II. DISTRIBUTION FUNCTION FOR PROTON AND NEUTRON NUMBERS

In this section, we discuss the time evolution of the proton and neutron number distributions in the hadronic medium generated by relativistic heavy ion collisions, and we show that the nucleon distribution in the final state in a phase space is factorized as in Eq. (2) at sufficiently large $\sqrt{s_{\rm NN}}$. In Sec. II A, as a preliminary example we show that Eq. (2) is applicable to the equilibrated free hadron gas in the ranges of T and $\mu_{\rm B}$ relevant to relativistic heavy ion collisions. We then extend the argument to the distribution function in the final state in relativistic heavy ion collisions in Sec. II B.

A. Free hadron gas in equilibrium

Let us first consider nucleons in the free hadron gas in equilibrium. For T and $\mu_{\rm B}$ which are relevant to relativistic heavy ion collisions, the nucleon mass $m_{\rm N}$ satisfies $m_{\rm N} - |\mu_{\rm B}| \gg T$. One thus can apply the Boltzmann approximation for the distribution functions of nucleons. The number of particles in a phase space, N, which obey Boltzmann statistics is given by the Poisson distribution,

$$P_\lambda(N) = \frac{e^{-\lambda}\lambda^N}{N!}, \tag{4}$$

with the average $\lambda = \langle N\rangle = \sum_N N P_\lambda(N)$. Accordingly, the probability of finding N_p ($N_{\bar p}$) protons (antiprotons) and N_n ($N_{\bar n}$) neutrons (antineutrons) in the phase space is given by the product of the Poisson distribution functions,

$$\begin{aligned}&\mathcal{P}_{\rm HG}(N_p, N_n, N_{\bar p}, N_{\bar n})\\ &\quad = P_{\langle N_p\rangle}(N_p)P_{\langle N_n\rangle}(N_n)P_{\langle N_{\bar p}\rangle}(N_{\bar p})P_{\langle N_{\bar n}\rangle}(N_{\bar n}).\end{aligned} \tag{5}$$

The product of two Poisson distribution functions satisfies the identity

$$\begin{aligned}&P_{\lambda_1}(N_1)P_{\lambda_2}(N_2)\\ &\quad = P_{\lambda_1+\lambda_2}(N_1+N_2)B_{\lambda_1/(\lambda_1+\lambda_2)}(N_1; N_1+N_2),\end{aligned} \tag{6}$$

where $B_r(k;n)$ is the binomial distribution function [Eq. (3)]. By using Eq. (6), Eq. (5) is rewritten as

$$\begin{aligned}&\mathcal{P}_{\rm HG}(N_p, N_n, N_{\bar p}, N_{\bar n})\\ &\quad = P_{\langle N_{\rm N}\rangle}(N_{\rm N})P_{\langle N_{\bar{\rm N}}\rangle}(N_{\bar{\rm N}})B_r(N_p; N_{\rm N})B_{\bar r}(N_{\bar p}; N_{\bar{\rm N}}),\end{aligned} \tag{7}$$

where $N_{\rm N} = N_p + N_n$ and $N_{\bar{\rm N}} = N_{\bar p} + N_{\bar n}$ are the nucleon and antinucleon numbers, respectively, and $r = \langle N_p\rangle/\langle N_{\rm N}\rangle$ and $\bar r = \langle N_{\bar p}\rangle/\langle N_{\bar{\rm N}}\rangle$. Equation (7) shows that the distribution of nucleons in the free hadron gas is factorized using binomial functions as in Eq. (2) with

$$\mathcal{F}(N_{\rm N}, N_{\bar{\rm N}}) = P_{\langle N_{\rm N}\rangle}(N_{\rm N})P_{\langle N_{\bar{\rm N}}\rangle}(N_{\bar{\rm N}}). \tag{8}$$

The appearance of the binomial distribution functions in Eq. (7) is understood as follows. When one finds a nucleon in the hadron gas, the probability that the nucleon is a proton is r. The isospins of all nucleons found in the phase space, moreover, are not correlated with one another as a consequence of Boltzmann statistics and the absence of interactions. Once $N_{\rm N}$ nucleons are found in the phase space, therefore, the probability that N_p particles are protons is a superposition of independent events with probability r, i.e., the binomial distribution.

We note that the above discussion is not applicable when the condition $m_{\rm N} - |\mu_{\rm B}| \gg T$, required for Boltzmann statistics, is not satisfied. When quantum correlations of nucleons arising from Fermi statistics are not negligible, the isospin of each nucleon can no longer be independent. As long as we are concerned with the range of T and $\mu_{\rm B}$ which can be realized by relativistic heavy ion collisions, however, the condition for the Boltzmann approximation is well satisfied except for very low energy collisions [26].

B. Final state in heavy ion collisions

Next, we consider the nucleon distribution functions in the final state in heavy ion collisions. We show that the nucleon distribution in this case is also factorized as in Eq. (2), by demonstrating that the isospins of all nucleons in the final state are random and uncorrelated.

1. **Δ(1232)** *resonance*

The key ingredient to obtain the factorization given by Eq. (2) in the final state in relativistic heavy ion collisions is Nπ reactions in the hadronic stage mediated by $\Delta(1232)$ resonances having isospin $I = 3/2$. As we will see later, this is the most dominant reaction of nucleons in the hadronic medium. This is because (i) the cross section of $\mathrm{N}\pi \to \Delta$ reactions exceeds 200 mb = 20 fm^2 and is comparable with that of NN and N$\bar{\rm N}$ reactions for $P_{\rm lab} \simeq 300$ MeV [27] and (ii) the pion density dominates over those of all other particles in the ranges of T and $\mu_{\rm B}$ accessible with heavy ion collisions at $\sqrt{s_{\rm NN}} \gtrsim 10$ GeV; at the top RHIC energy, the density of pions is more than one order larger than that of nucleons. We shall show below that these reactions frequently take place even after chemical freeze-out in the hadronic medium during the time evolution of the fireballs.

The Nπ reactions through the Δ contain charge exchange reactions, which alter the isospin of the nucleon in the reaction. The reactions of a proton to form the Δ are

$$p + \pi^+ \to \Delta^{++} \to p + \pi^+, \tag{9}$$

$$p + \pi^0 \to \Delta^+ \to p(n) + \pi^0(\pi^+), \tag{10}$$

$$p + \pi^- \to \Delta^0 \to p(n) + \pi^-(\pi^0). \tag{11}$$

Among these reactions, Eqs. (10) and (11) are responsible for the change of the nucleon isospin. The ratio of the cross sections of a proton to form Δ^{++}, Δ^+, and Δ^0 is 3:1:2, which is determined by the isospin SU(2) symmetry of the strong interaction. The isospin symmetry also tells us that the branching ratios of Δ^+ (Δ^0) decaying into the final state having a proton and a neutron are 1:2 (2:1). Using these ratios, one obtains the ratio of the probabilities that a proton in the hadron gas forms Δ^+ or Δ^0 with a reaction with a thermal pion, and then decays into a proton and a neutron, respectively, $P_{p\to p}$ and $P_{p\to n}$, as

$$P_{p\to p} : P_{p\to n} = 5 : 4, \tag{12}$$

provided that the hadronic medium is isospin symmetric and that the three isospin states of the pion are equally distributed in the medium. Because of the isospin symmetry of the strong interaction one also obtains the same conclusion for neutron reactions:

$$P_{n\to n} : P_{n\to p} = 5 : 4. \tag{13}$$

Similar results are also obtained for antinucleons. Equations (12) and (13) show that these reactions act to randomize the isospin of nucleons during the hadronic stage.

2. *Mean time*

Next, let us estimate the mean time of these reactions. By assuming that pions are thermally distributed, the mean time τ_Δ of a nucleon at rest in the medium to undergo a reaction via Eq. (10) or (11) is given by

$$\tau_\Delta^{-1} = \int \frac{d^3k_\pi}{(2\pi)^3}\sigma(E_{\rm c.m.})v_\pi n(E_\pi), \tag{14}$$

with the Bose distribution function $n(E) = (e^{E/T} - 1)^{-1}$, the pion momentum k_π, the pion velocity $v_\pi = k_\pi/E_\pi$, $E_\pi = \sqrt{m_\pi^2 + k_\pi^2}$, and the pion mass m_π. $\sigma(E_{\rm c.m.})$ is the sum of the cross sections for Nπ reactions producing Δ^+ and Δ^0 for the center-of-mass energy $E_{\rm c.m.} = [(m_{\rm N} + E_\pi)^2 - k_\pi^2]^{1/2}$ with nucleon mass $m_{\rm N}$. For the cross section $\sigma(E_{\rm c.m.})$, we assume that the peak corresponding to the $\Delta(1232)$ resonance is well reproduced by the Breit-Wigner form

$$\sigma(E_{\rm c.m.}) = \sigma_\Delta \frac{\Gamma^2/4}{(E_{\rm c.m.} - m_\Delta)^2 + \Gamma^2/4}, \tag{15}$$

which is a sufficient approximation for our purpose. Here, we use the value of the parameters determined by the Nπ reactions in vacuum, $m_\Delta = 1232$ MeV, $\Gamma = 110$ MeV, and $\sigma_\Delta = 20$ fm^2 [27]. The medium effects on the cross section will be discussed later. Substituting $m_{\rm N} = 940$ MeV and $m_\pi = 140$ MeV, one obtains the T dependence of the mean time τ_Δ presented in Fig. 1. The figure shows that the mean time is $\tau_\Delta = 3$–4 fm for $T = 150$–170 MeV. One can confirm that

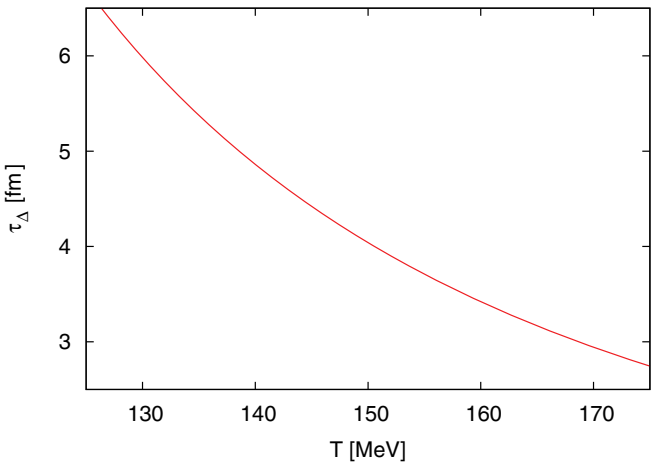

FIG. 1. (Color online) Mean time τ_Δ of a rest nucleon to form Δ^+ or Δ^0 in the hadronic medium as a function of temperature T.

the mean time hardly changes even for moving nucleons in the range of momentum $p \lesssim 3T$ by extending Eq. (14) to cases with nonzero nucleon momentum. The lifetime of Δ resonances is $\tau_\Gamma = 1/\Gamma \simeq 1.8$ fm.

The mean time evaluated above is much shorter than the lifetime of the hadronic stage in relativistic heavy ion collisions. According to a dynamical model analysis for collisions at the RHIC, nucleons in the hadron phase continue to interact for a couple of tens of femtometers on average at midrapidity [28]. As a result, at the RHIC energy each nucleon in a fireball has chances to undergo charge exchange reactions several times in the hadronic stage.

Two remarks are in order here. First, the above result on the time scales shows that the reactions to produce the Δ proceed even after chemical freeze-out. These reactions do not contradict the success of the statistical model, which describes chemical freeze-out [29], because chemical freeze-out is a concept to describe ratios of particle abundances such as $\langle N_{\bar p}\rangle/\langle N_p\rangle$ and the above reactions do not alter the average abundances in the final state. The success of the model, on the other hand, indicates that creation and annihilation of (anti)nucleons hardly occur after chemical freeze-out. Second, we note that the dynamical model in Ref. [28] uses an equation of state having a first-order phase transition in the hydrodynamic simulations for the time evolution above the critical temperature $T_{\rm c}$. Recently, dynamical simulations have been carried out with more realistic equations of state obtained by lattice QCD simulations [30]. The lifetime of the hadronic stage evaluated in these studies is more relevant to this argument. We, however, note that the qualitative behavior of the time evolution seems to be insensitive to the difference in equations of state [30].

While Nπ reactions frequently take place even below the chemical freeze-out temperature, $T_{\rm chem}$, N$\bar{\rm N}$ annihilation and production almost terminate at $T_{\rm chem}$. This is necessary for the success of the thermal model. For $E_{\rm c.m.} \simeq T$ the cross section of the N$\bar{\rm N}$ pair annihilation is largest among all NN and N$\bar{\rm N}$ reactions. If nucleons and antinucleons are distributed without correlation, therefore, all NN and N$\bar{\rm N}$ reactions cease to take place at $T_{\rm chem}$. This conclusion is, of course, obtained also by evaluating the mean time for each reaction using the cross sections [27] as in Eq. (14). After chemical freeze-out, the only inelastic reactions nucleons go through are thus Eqs. (10) and (11), and after each reaction the nucleon loses its initial isospin information. Only after repeating the reactions of Eq. (12) twice, the ratio becomes 41:40, which is almost even. If medium effects on the formation and decay of the Δ are negligible, therefore, irrespective of the nucleon distribution at chemical freeze-out, the isospin of nucleons at kinetic freeze-out can be regarded as random and uncorrelated. On the other hand, the nucleon number distribution can deviate from the Boltzmann distribution, reflecting the dynamical history of fireballs.

Because of the absence of correlations between isospins of nucleons in the final state, once $N_{\rm N}$ ($N_{\bar{\rm N}}$) nucleons (antinucleons) exist in a phase space in the final state, their isospin distribution is simply given by the binomial one. This conclusion leads to the factorization Eq. (2) for proton and neutron number distribution in the final state for an arbitrary

phase space. In particular, the final state proton and antiproton number distribution is written as

$$\mathcal{G}(N_p, N_{\bar{p}}) = \sum_{N_n, N_{\bar{n}}} \mathcal{P}_{\rm N}(N_p, N_n, N_{\bar{p}}, N_{\bar{n}}) = \sum_{N_{\rm N}, N_{\bar{\rm N}}} \mathcal{F}(N_{\rm N}, N_{\bar{\rm N}}) B_r(N_p; N_{\rm N}) B_{\bar{r}}(N_{\bar{p}}; N_{\bar{\rm N}}). \quad (16)$$

Unlike in the simple example in Sec. II A, the nucleon distribution function $\mathcal{F}(N_{\rm N}, N_{\bar{\rm N}})$ in this case is determined by the time evolution of fireballs and is not necessarily of a thermal or separable form as in Eq. (8); no specific form for $\mathcal{F}(N_{\rm N}, N_{\bar{\rm N}})$ is assumed here or will be assumed in the analyses in Sec. III. What we have used here is the fact that the time scale for the exchange of isospins between nucleons and pions is sufficiently short compared to the lifetime of the hadronic stage after chemical freeze-out. On the other hand, the time scale for the variation of conserved charge in a phase space depends on the form of the phase space, and it can become arbitrary long by increasing the spatial volume. When the time scale is long, information of the physics of the early stages is encoded in $\mathcal{F}(N_{\rm N}, N_{\bar{\rm N}})$.

3. *Medium effects*

Next, let us inspect the possibility of medium effects on the formation and decay rates of the Δ. In medium, the decay rate of the Δ acquires the statistical factor

$$[1 - f(E_{\rm N})]\,[1 + n(E_\pi)]\,, \quad (17)$$

where $f(E) = (e^{(E-\mu_{\rm B})/T} + 1)^{-1}$ is the Fermi distribution function and $E_{\rm N}$ and E_π are the energies of the nucleon and pion produced by the decay, respectively. The first term in Eq. (17) represents the Pauli blocking effect. At the RHIC energy, since the Boltzmann approximation is well applied to nucleons, the Pauli blocking effect is suppressed. The Bose factor $[1 + n(E_\pi)]$ in Eq. (17), on the other hand, has a non-negligible contribution since $m_\pi \simeq T_{\rm chem}$. As long as all $n(E_\pi)$ for the three isospin states of the pion are the same, however, this factor does not alter the branching ratios given by Eqs. (12) and (13), while the factor enhances the decay of the Δ. A possible origin for the variation of $n(E_\pi)$ is the isospin density of nucleon number; since the isospin density is locally conserved, the isospin density of pions is affected by the nucleon isospin. This effect on $n(E_\pi)$ is, however, well suppressed since the density of pions is much larger than that of nucleons below $T_{\rm chem}$. Another possible source which gives rise to a different pion distribution is the event-by-event fluctuation of the isospin density in the phase space at hadronization. It is, however, expected that the effect is well suppressed, again because of the large pion density. One, therefore, can conclude that the medium effect hardly changes the branching ratios Eqs. (12) and (13). The same conclusion also applies to the formation rate of the Δ, since the medium effect on the probabilities of a nucleon to undergo reactions Eqs. (9)–(11) depends only on $n(E_\pi)$. After all, all medium effects on the ratios Eqs. (12) and (13) are negligible.

When the system has a nonzero isospin density, the probabilities in Eqs. (12) and (13) receive modifications because the three isospin states of the pion are not equally distributed, although this effect is not large, as will be shown in Sec. III D. Even in this case, however, the only modification to the above conclusion is to replace the probabilities r and $\bar{r}$ with appropriate values, since the reactions given by Eqs. (9)–(11) still act to randomize the nucleon isospins with the modified probabilities determined by the detailed balance condition.

Here, we emphasize that the large pion density in the hadronic medium is responsible for the validity of Eq. (16) in the final state. In the hadronic medium, there are so many pions and they can be regarded as a heat bath when the nucleon sector is concerned, while nucleons are so dilutely distributed that they do not feel each other's existence.

So far, we have limited our attention to reactions mediated by $\Delta(1232)$. Interactions of nucleons with other mesons, however, can also take place in the hadronic medium, while they are much less dominant. It is also possible that the Δ interacts with thermal pions to form another resonance before its decay [31]. All these reactions with thermal particles, however, proceed with certain probabilities determined by the isospin SU(2) symmetry as long as they are caused by the strong interaction. Each reaction of a nucleon thus makes its isospin random and acts to realize the factorization Eq. (2).

4. *Low-beam-energy region*

The factorization given by Eq. (16) is fully established for the RHIC energy. At very low beam energy, however, pions are not produced enough and the duration of the hadron phase below $T_{\rm chem}$ becomes shorter. Nucleons, therefore, will not undergo sufficient charge exchange reactions below $T_{\rm chem}$. When the reactions hardly occur, the isospin correlations generated at the hadronization remain until the final state. At low beam energy, also the density of the nucleon becomes comparable to that of pions, and pions can no longer be regarded as a heat bath to absorb isospin fluctuations of nucleons. The requirements to justify the factorization given by Eq. (16), therefore, eventually breaks down as the beam energy is decreased. This would happen when $T_{\rm chem} \lesssim m_\pi$, since the abundance of pions is responsible for all of the above conditions. From the $\sqrt{s_{\rm NN}}$ dependence of the chemical freeze-out line on the T-$\mu_{\rm B}$ plane [26], the factorization given by Eq. (16) should be well satisfied in the range of beam energy $\sqrt{s_{\rm NN}} \gtrsim 10$ GeV.

C. Strange baryons

So far, we have limited our attention to nucleons. Since baryons in the final state in heavy ion collisions are dominated by nucleons, the nucleon number, which is not a conserved charge, is qualitatively identified with the baryon one. It is, however, important to recognize the difference between these two fluctuation observables especially in considering higher order cumulants. The difference predominantly comes from the strange baryons Λ and Σ. In this section, we argue a practical method to include the effect of these degrees of freedom in our factorization formula.

Strange baryons produced in the hadronic medium decay via the weak or electromagnetic interaction outside the fireball. The Λ decays via the weak interaction into $p\pi^-$ and $n\pi^0$ with the branching ratio

$$P_{\Lambda\to p} : P_{\Lambda\to n} \simeq 16 : 9. \tag{18}$$

On the other hand, the branching ratio of Σ^+ is

$$P_{\Sigma^+\to p} : P_{\Sigma^+\to n} \simeq 13 : 12, \tag{19}$$

while Σ^- always decays into $n\pi^-$. Σ^0 decays into a Λ via the electromagnetic interaction and then decays with Eq. (18) [27]. If the Λ and Σ multiplets are created with an equal probability, the production ratio of p and n from their decays is given by

$$P_{\Lambda,\Sigma\to p} : P_{\Lambda,\Sigma\to n} \simeq 9 : 11. \tag{20}$$

Actually, because of the mass splitting between the Λ and the Σ triplets, $\delta m \simeq T_{\rm chem}/2$, the production of the Σ triplets are a bit suppressed compared to that of the Λ. This makes the above ratio even closer to even. If one can assume that the correlations between strange baryons emitted from the fireball are negligible, therefore, the number of nucleons produced by these decays can be incorporated into N_p and N_n in Eq. (2). The nucleon number in Eq. (2), then, is promoted to that of baryons. The same argument holds also for the antiparticles $\bar\Lambda$ and $\bar\Sigma$.

In short, by simply counting all protons observed by detectors in the event-by-event analysis, $N_{\rm N}$ and $N_{\bar{\rm N}}$ in Eq. (2) are automatically promoted to the baryon and antibaryon numbers, respectively.

III. RELATING BARYON AND PROTON NUMBER CUMULANTS

In this section, we focus on the cumulants of the baryon and proton numbers, and we derive formulas to relate these cumulants on the basis of the factorization given by Eq. (2). With these relations the cumulants of the baryon number, which is a conserved charge, are calculated from experimentally observed proton number ones.

In this section, we change the variables in the probability distribution function in Eq. (2) as

$$\mathcal{P}(N_p, N_{\bar p}; N_{\rm B}, N_{\bar{\rm B}}) = \mathcal{P}_N(N_p, N_n, N_{\bar p}, N_{\bar n}), \tag{21}$$

where we have replaced the neutron numbers with the baryon ones, $N_{\rm B} = N_p + N_n$ and $N_{\bar{\rm B}} = N_{\bar p} + N_{\bar n}$. It is understood that the prescription discussed in Sec. II C is adopted for Λ, Σ, and their antiparticles.

A. Probability distribution functions

Before deriving formulas to relate the baryon and proton number cumulants, in this section we first remark that the distribution functions of these degrees of freedom satisfy a linear relation under the factorization given by Eq. (2). This relation explains why the baryon number cumulants can be represented by the proton number cumulants and vice versa.

Let us start with the final state proton and antiproton number distribution function, Eq. (16),

$$\begin{aligned}\mathcal{G}(N_p, N_{\bar p}) &= \sum_{N_{\rm B}, N_{\bar{\rm B}}} \mathcal{P}(N_p, N_{\bar p}; N_{\rm B}, N_{\bar{\rm B}}) \\ &= \sum_{N_{\rm B}, N_{\bar{\rm B}}} \mathcal{F}(N_{\rm B}, N_{\bar{\rm B}}) M(N_p, N_{\bar p}; N_{\rm B}, N_{\bar{\rm B}})\end{aligned} \tag{22}$$

with

$$M(N_p, N_{\bar p}; N_B, N_{\bar{\rm B}}) = B_r(N_p; N_{\rm B}) B_{\bar r}(N_{\bar p}; N_{\bar{\rm B}}). \tag{23}$$

Equation (22) shows that the distribution functions $\mathcal{G}(N_p, N_{\bar p})$ and $\mathcal{F}(N_{\rm B}, N_{\bar{\rm B}})$ satisfy a linear relation. Since $M(N_p, N_{\bar p}; N_{\rm B}, N_{\bar{\rm B}})$ has the inverse $M^{-1}(N_B, N_{\bar B}; N_p, N_{\bar p})$, $\mathcal{F}(N_{\rm B}, N_{\bar{\rm B}})$ is given in terms of $\mathcal{G}(N_p, N_{\bar p})$ as

$$\mathcal{F}(N_{\rm B}, N_{\bar{\rm B}}) = \sum_{N_p, N_{\bar p}} \mathcal{G}(N_p, N_{\bar p}) M^{-1}(N_{\rm B}, N_{\bar{\rm B}}; N_p, N_{\bar p}). \tag{24}$$

The specific form of $M^{-1}(N_{\rm B}, N_{\bar{\rm B}}; N_p, N_{\bar p})$ is easily obtained by using the fact that the matrix given by Eq. (23) has a triangular structure, in the sense that $M(N_p, N_{\bar p}; N_{\rm B}, N_{\bar{\rm B}})$ takes nonzero values only for $N_p \leqslant N_{\rm B}$ and $N_{\bar p} \leqslant N_{\bar{\rm B}}$. By using Eq. (24), the baryon number distribution function $\mathcal{F}(N_{\rm B}, N_{\bar{\rm B}})$ [32] is in principle determined by $\mathcal{G}(N_p, N_{\bar p})$. In practice, however, this analysis does not work efficiently since the elements of $M^{-1}(N_{\rm B}, N_{\bar{\rm B}}; N_p, N_{\bar p})$ are rapidly oscillating, which results in large error bars in $\mathcal{F}(N_{\rm B}, N_{\bar{\rm B}})$ determined in this way. In the following, instead of the distribution functions themselves, we concentrate on the cumulants of $\mathcal{F}(N_{\rm B}, N_{\bar{\rm B}})$ and $\mathcal{G}(N_p, N_{\bar p})$.

B. Generating functions and cumulants

The moments and cumulants of a distribution function are defined in terms of their generating functions. The moment-generating function for the proton and antiproton numbers with probability $\mathcal{P}(N_p, N_{\bar p}; N_{\rm B}, N_{\bar{\rm B}})$ is given by

$$G(\theta, \bar\theta) = \sum_{N_p, N_{\bar p}, N_{\rm B}, N_{\bar{\rm B}}} \mathcal{P}(N_p, N_{\bar p}; N_{\rm B}, N_{\bar{\rm B}}) e^{N_p\theta} e^{N_{\bar p}\bar\theta}, \tag{25}$$

and the corresponding cumulant generating function reads

$$K(\theta, \bar\theta) = \log G(\theta, \bar\theta). \tag{26}$$

Derivatives of Eq. (25) give moments of $\mathcal{P}(N_p, N_{\bar p}; N_{\rm B}, N_{\bar{\rm B}})$:

$$\left\langle N_p^n N_{\bar p}^m \right\rangle = \frac{\partial^n}{\partial\theta^n} \frac{\partial^m}{\partial\bar\theta^m} G(\theta, \bar\theta)\bigg|_{\theta=\bar\theta=0}, \tag{27}$$

as long as the sum in Eq. (25) converges, while cumulants of the proton and antiproton numbers are defined with Eq. (26) as

$$\langle (\delta N_p)^n (\delta N_{\bar p})^m \rangle_c = \frac{\partial^n}{\partial\theta^n} \frac{\partial^m}{\partial\bar\theta^m} K(\theta, \bar\theta)\bigg|_{\theta=\bar\theta=0}. \tag{28}$$

The first-order cumulant is the expectation value of the operator,

$$\langle \delta N_p \rangle_c = \langle N_p \rangle, \quad \langle \delta N_{\bar p} \rangle_c = \langle N_{\bar p} \rangle, \tag{29}$$

while the second- and third-order cumulants are moments of fluctuations, such as

$$\langle \delta N_p \delta N_{\bar{p}} \rangle_c = \langle \delta N_p \delta N_{\bar{p}} \rangle, \tag{30}$$

and so forth, with $\delta N_X = N_X - \langle N_X \rangle$.

Substituting the explicit form of $\mathcal{P}(N_p, N_{\bar{p}}; N_{\rm B}, N_{\bar{\rm B}})$ in Eq. (16) for $K(\theta, \bar{\theta})$, one obtains

$$K(\theta, \bar{\theta}) = \log \sum_{N_{\rm B}, N_{\bar{\rm B}}} \mathcal{F}(N_{\rm B}, N_{\bar{\rm B}}) \exp[k_{N_{\rm B}, N_{\bar{\rm B}}}(\theta, \bar{\theta})], \tag{31}$$

where

$$k_{N_{\rm B}, N_{\bar{\rm B}}}(\theta, \bar{\theta}) = \log \sum_{N_p} B_r(N_p; N_{\rm B}) e^{N_p \theta} + \log \sum_{N_{\bar{p}}} B_{\bar{r}}(N_{\bar{p}}; N_{\bar{\rm B}}) e^{N_{\bar{p}} \bar{\theta}} \tag{32}$$

is the cumulant-generating function for two independent binomial distribution functions. With Eq. (32), one easily finds that this function satisfies $k_{N_{\rm B}, N_{\bar{\rm B}}}(0, 0) = 0$ and

$$\frac{\partial^n}{\partial \theta^n} k_{N_{\rm B}, N_{\bar{\rm B}}}(0, 0) = \xi_n N_{\rm B}, \tag{33}$$

$$\frac{\partial^m}{\partial \bar{\theta}^m} k_{N_{\rm B}, N_{\bar{\rm B}}}(0, 0) = \bar{\xi}_m N_{\bar{\rm B}}, \tag{34}$$

$$\frac{\partial^{n+m}}{\partial \theta^n \partial \bar{\theta}^m} k_{N_{\rm B}, N_{\bar{\rm B}}}(0, 0) = 0, \tag{35}$$

for positive integers n and m, with the cumulants of the binomial distribution function normalized by the total number,

$$\xi_1 = r, \quad \xi_2 = r(1-r), \quad \xi_3 = r(1-r)(1-2r), \quad \xi_4 = r(1-r)(1-6r+6r^2), \ \cdots, \tag{36}$$

and the same formulas for the antiparticle sector. By imposing Eqs. (31)–(35) as the structure of $K(\theta, \bar{\theta})$, cumulants of net proton and baryon numbers, $N_p^{(\rm net)} = N_p - N_{\bar{p}}$ and $N_{\rm B}^{(\rm net)} = N_{\rm B} - N_{\bar{\rm B}}$, respectively, are calculated to be

$$\langle N_p^{(\rm net)} \rangle = \langle \xi_1 N_{\rm B} - \bar{\xi}_1 N_{\bar{\rm B}} \rangle, \tag{37}$$

$$\langle (\delta N_p^{(\rm net)})^2 \rangle = \langle (\xi_1 \delta N_{\rm B} - \bar{\xi}_1 \delta N_{\bar{\rm B}})^2 \rangle + \langle \xi_2 N_{\rm B} + \bar{\xi}_2 N_{\bar{\rm B}} \rangle, \tag{38}$$

$$\langle (\delta N_p^{(\rm net)})^3 \rangle = \langle (\xi_1 \delta N_{\rm B} - \bar{\xi}_1 \delta N_{\bar{\rm B}})^3 \rangle + 3\langle (\xi_2 \delta N_{\rm B} + \bar{\xi}_2 \delta N_{\bar{\rm B}})(\xi_1 \delta N_{\rm B} - \bar{\xi}_1 \delta N_{\bar{\rm B}}) \rangle + \langle \xi_3 N_{\rm B} - \bar{\xi}_3 N_{\bar{\rm B}} \rangle, \tag{39}$$

$$\langle (\delta N_p^{(\rm net)})^4 \rangle_c = \langle (\xi_1 \delta N_{\rm B} - \bar{\xi}_1 \delta N_{\bar{\rm B}})^4 \rangle_c + 6\langle (\xi_2 \delta N_{\rm B} + \bar{\xi}_2 \delta N_{\bar{\rm B}})(\xi_1 \delta N_{\rm B} - \bar{\xi}_1 \delta N_{\bar{\rm B}})^2 \rangle + 3\langle (\xi_2 \delta N_{\rm B} + \bar{\xi}_2 \delta N_{\bar{\rm B}})^2 \rangle + 4\langle (\xi_3 \delta N_{\rm B} - \bar{\xi}_3 \delta N_{\bar{\rm B}})(\xi_1 \delta N_{\rm B} - \bar{\xi}_1 \delta N_{\bar{\rm B}}) \rangle + \langle \xi_4 N_{\rm B} + \bar{\xi}_4 N_{\bar{\rm B}} \rangle \tag{40}$$

and

$$\langle N_{\rm B}^{(\rm net)} \rangle = \langle \xi_1^{-1} N_p - \bar{\xi}_1^{-1} N_{\bar{p}} \rangle, \tag{41}$$

$$\langle (\delta N_{\rm B}^{(\rm net)})^2 \rangle = \langle (\xi_1^{-1} \delta N_p - \bar{\xi}_1^{-1} \delta N_{\bar{p}})^2 \rangle - \langle \xi_2 \xi_1^{-3} \delta N_p + \bar{\xi}_2 \bar{\xi}_1^{-3} \delta N_{\bar{p}} \rangle, \tag{42}$$

$$\langle (\delta N_{\rm B}^{(\rm net)})^3 \rangle = \langle (\xi_1^{-1} \delta N_p - \bar{\xi}_1^{-1} \delta N_{\bar{p}})^3 \rangle - 3\langle (\xi_2 \xi_1^{-3} \delta N_p + \bar{\xi}_2 \bar{\xi}_1^{-3} \delta N_{\bar{p}})(\xi_1^{-1} \delta N_p - \bar{\xi}_1^{-1} \delta N_{\bar{p}}) \rangle + \left\langle \frac{3\xi_2^2 - \xi_1 \xi_3}{\xi_1^5} N_p - \frac{3\bar{\xi}_2^2 - \bar{\xi}_1 \bar{\xi}_3}{\bar{\xi}_1^5} N_{\bar{p}} \right\rangle, \tag{43}$$

$$\langle (\delta N_{\rm B}^{(\rm net)})^4 \rangle_c = \langle (\xi_1^{-1} \delta N_p - \bar{\xi}_1^{-1} \delta N_{\bar{p}})^4 \rangle_c - 6\langle (\xi_2 \xi_1^{-3} \delta N_p + \bar{\xi}_2 \bar{\xi}_1^{-3} \delta N_{\bar{p}})(\xi_1^{-1} \delta N_p - \bar{\xi}_1^{-1} \delta N_{\bar{p}}) \rangle + 12\langle (\xi_2^2 \xi_1^{-5} \delta N_p - \bar{\xi}_2^2 \bar{\xi}_1^{-5} \delta N_{\bar{p}}) \times (\xi_1^{-1} \delta N_p - \bar{\xi}_1^{-1} \delta N_{\bar{p}}) \rangle + 3\langle (\xi_2 \xi_1^{-3} \delta N_p + \bar{\xi}_2 \bar{\xi}_1^{-3} \delta N_{\bar{p}})^2 \rangle - 4\langle (\xi_3 \xi_1^{-4} \delta N_p - \bar{\xi}_3 \bar{\xi}_1^{-4} \delta N_{\bar{p}})(\xi_1^{-1} \delta N_p - \bar{\xi}_1^{-1} \delta N_{\bar{p}}) \rangle - \left\langle \frac{15\xi_2^3 - 10\xi_1 \xi_2 \xi_3 + \xi_1^2 \xi_4}{\xi_1^7} N_p - \frac{15\bar{\xi}_2^3 - 10\bar{\xi}_1 \bar{\xi}_2 \bar{\xi}_3 + \bar{\xi}_1^2 \bar{\xi}_4}{\bar{\xi}_1^7} N_{\bar{p}} \right\rangle. \tag{44}$$

A detailed description of the procedure to obtain these results is given in Appendix A. We emphasize that no explicit form of $\mathcal{F}(N_{\rm B}, N_{\bar{\rm B}})$ is assumed in deriving these results. Moreover, in Appendix A we only use Eq. (31) for the structure of $K(\theta, \bar{\theta})$ and Eqs. (33)–(35) for properties of $k_{N_{\rm B}, N_{\bar{\rm B}}}(\theta, \bar{\theta})$ to derive Eqs. (37)–(44). Therefore, these results hold for any distribution functions satisfying these conditions with the appropriate choice for the values of ξ_i and $\bar{\xi}_i$.

C. Isospin-symmetric case

In a hot medium produced by heavy ion collisions, (anti)proton and (anti)neutron number densities are in general different because of the isospin asymmetry of colliding heavy nuclei. In relativistic heavy ion collisions at sufficiently large $\sqrt{s_{\rm NN}}$ and small impact parameters, however, the isospin density is negligibly small because a large number of particles having nonzero isospin charges (mainly pions) are created and most of the initial isospin density is absorbed by these degrees of freedom (see Appendix B). When the isospin density vanishes, r and $\bar{r}$ are to be set at $1/2$ in the binomial distribution functions in Eq. (2). Substituting

$$\xi_1 = \tfrac{1}{2}, \quad \xi_2 = \tfrac{1}{4}, \quad \xi_3 = 0, \quad \xi_4 = -\tfrac{1}{8} \tag{45}$$

into Eqs. (37)–(44), which are obtained by putting $r = 1/2$ in Eq. (36), one obtains

$$\langle N_p^{(\mathrm{net})}\rangle = \tfrac{1}{2}\langle N_{\mathrm{B}}^{(\mathrm{net})}\rangle, \tag{46}$$

$$\langle (\delta N_p^{(\mathrm{net})})^2\rangle = \tfrac{1}{4}\langle (\delta N_{\mathrm{B}}^{(\mathrm{net})})^2\rangle + \tfrac{1}{4}\langle N_{\mathrm{B}}^{(\mathrm{tot})}\rangle, \tag{47}$$

$$\langle (\delta N_p^{(\mathrm{net})})^3\rangle = \tfrac{1}{8}\langle (\delta N_{\mathrm{B}}^{(\mathrm{net})})^3\rangle + \tfrac{3}{8}\langle \delta N_{\mathrm{B}}^{(\mathrm{net})}\delta N_{\mathrm{B}}^{(\mathrm{tot})}\rangle, \tag{48}$$

$$\langle (\delta N_p^{(\mathrm{net})})^4\rangle_c = \tfrac{1}{16}\langle (\delta N_{\mathrm{B}}^{(\mathrm{net})})^4\rangle_c + \tfrac{3}{8}\langle (\delta N_{\mathrm{B}}^{(\mathrm{net})})^2\delta N_{\mathrm{B}}^{(\mathrm{tot})}\rangle + \tfrac{3}{16}\langle (\delta N_{\mathrm{B}}^{(\mathrm{tot})})^2\rangle - \tfrac{1}{8}\langle N_{\mathrm{B}}^{(\mathrm{tot})}\rangle \tag{49}$$

and

$$\langle N_{\mathrm{B}}^{(\mathrm{net})}\rangle = 2\langle N_p^{(\mathrm{net})}\rangle, \tag{50}$$

$$\langle (\delta N_{\mathrm{B}}^{(\mathrm{net})})^2\rangle = 4\langle (\delta N_p^{(\mathrm{net})})^2\rangle - 2\langle N_p^{(\mathrm{tot})}\rangle, \tag{51}$$

$$\langle (\delta N_{\mathrm{B}}^{(\mathrm{net})})^3\rangle = 8\langle (\delta N_p^{(\mathrm{net})})^3\rangle - 12\langle \delta N_p^{(\mathrm{net})}\delta N_p^{(\mathrm{tot})}\rangle + 6\langle N_p^{(\mathrm{net})}\rangle, \tag{52}$$

$$\langle (\delta N_{\mathrm{B}}^{(\mathrm{net})})^4\rangle_c = 16\langle (\delta N_p^{(\mathrm{net})})^4\rangle_c - 48\langle (\delta N_p^{(\mathrm{net})})^2\delta N_p^{(\mathrm{tot})}\rangle + 48\langle (\delta N_p^{(\mathrm{net})})^2\rangle + 12\langle (\delta N_p^{(\mathrm{tot})})^2\rangle - 26\langle N_p^{(\mathrm{tot})}\rangle, \tag{53}$$

which are the results given in Ref. [25]. Here a note is in order about the terms on the right-hand sides (RHSs) of Eqs. (51)–(53). Each term on the RHS of these equations is not necessarily uncorrelated with each other. In particular, generally $\mathcal{F}(N_{\mathrm{B}}, N_{\bar{\mathrm{B}}})$ is not separable; i.e., it cannot be written as $\mathcal{F}(N_{\mathrm{B}}, N_{\bar{\mathrm{B}}}) = f(N_{\mathrm{B}})g(N_{\bar{\mathrm{B}}})$. If there is such a correlation, the statistical fluctuations of these terms are not independent but mutually correlated. Thus, appropriate care needs to be taken in estimating the statistical error for the LHSs of Eqs. (51)–(53).

D. Effect of nonzero isospin density

As the collision energy is lowered, the effect of nonzero isospin density eventually gives rise to a non-negligible contribution to the above relations. To investigate this effect, we first assume that the isospins of nucleons, antinucleons, and pions in the final state are in chemical equilibrium, as is indicated by the fast Nπ reactions discussed in the previous section. Because the nucleon distribution is well approximated by the Boltzmann distribution, the numbers of (anti)protons and (anti)neutrons in the final state are given with isospin chemical potential μ_{I} and temperature T as

$$\begin{aligned} \langle N_p\rangle &= Ce^{\mu_{\mathrm{I}}/(2T)}, \quad \langle N_{\bar{p}}\rangle = De^{-\mu_{\mathrm{I}}/(2T)}, \\ \langle N_n\rangle &= Ce^{-\mu_{\mathrm{I}}/(2T)}, \quad \langle N_{\bar{n}}\rangle = De^{\mu_{\mathrm{I}}/(2T)}, \end{aligned} \tag{54}$$

where C and D are constants determined by the chemical freeze-out condition such as the volume of the system, the rapidity coverage, and so on. These relations lead to

$$\frac{\langle N_p\rangle}{\langle N_n\rangle} = \frac{\langle N_{\bar{n}}\rangle}{\langle N_{\bar{p}}\rangle} = e^{\mu_{\mathrm{I}}/T}, \tag{55}$$

and thereby $r = 1 - \bar{r}$. One thus can parametrize r and $\bar{r}$ as

$$r = \tfrac{1}{2} - \alpha, \quad \bar{r} = \tfrac{1}{2} + \alpha, \tag{56}$$

with the negative isospin density per nucleon,

$$\alpha = \frac{1}{2}\frac{\langle N_n\rangle - \langle N_p\rangle}{\langle N_n\rangle + \langle N_p\rangle} = \frac{1}{2}\frac{1 - e^{\mu_{\mathrm{I}}/T}}{1 + e^{\mu_{\mathrm{I}}/T}}. \tag{57}$$

α assumes a positive value in heavy ion collisions.

When the value of α is small ($\alpha \ll 1$), the effects of nonzero isospin density on Eqs. (41)–(44) are well described by the Taylor series with respect to α. By substituting Eq. (56) in these equations, up to first order in α Eqs. (50)–(53) become

$$\langle N_{\mathrm{B}}^{(\mathrm{net})}\rangle = 2\langle N_p^{(\mathrm{net})}\rangle + 4\alpha\langle N_p^{(\mathrm{tot})}\rangle + O(\alpha^2), \tag{58}$$

$$\langle (\delta N_{\mathrm{B}}^{(\mathrm{net})})^2\rangle = 4\langle (\delta N_p^{(\mathrm{net})})^2\rangle + 2\langle N_p^{(\mathrm{tot})}\rangle + 4\alpha\left[4\langle \delta N_p^{(\mathrm{net})}\delta N_p^{(\mathrm{tot})}\rangle - 3\langle N_p^{(\mathrm{net})}\rangle\right] + O(\alpha^2), \tag{59}$$

$$\langle (\delta N_{\mathrm{B}}^{(\mathrm{net})})^3\rangle = 8\langle (\delta N_p^{(\mathrm{net})})^3\rangle - 12\langle \delta N_p^{(\mathrm{net})}\delta N_p^{(\mathrm{tot})}\rangle + 6\langle N_p^{(\mathrm{net})}\rangle + 4\alpha\left[12\langle (\delta N_p^{(\mathrm{net})})^2\delta N_p^{(\mathrm{tot})}\rangle - 18\langle (\delta N_p^{(\mathrm{net})})^2\rangle - 6\langle (\delta N_p^{(\mathrm{toe})})^2\rangle + 13\langle N_p^{(\mathrm{tot})}\rangle\right] + O(\alpha^2), \tag{60}$$

$$\langle (\delta N_{\mathrm{B}}^{(\mathrm{net})})^4\rangle_c = 16\langle (\delta N_p^{(\mathrm{net})})^4\rangle_c - 48\langle (\delta N_p^{(\mathrm{net})})^2\delta N_p^{(\mathrm{tot})}\rangle + 48\langle (\delta N_p^{(\mathrm{net})})^2\rangle + 12\langle (\delta N_p^{(\mathrm{tot})})^2\rangle - 26\langle N_p^{(\mathrm{tot})}\rangle + 4\alpha\left[32\langle (\delta N_p^{(\mathrm{net})})^3\delta N_p^{(\mathrm{tot})}\rangle_c - 72\langle (\delta N_p^{(\mathrm{net})})^3\rangle - 48\langle \delta N_p^{(\mathrm{net})}(\delta N_p^{(\mathrm{tot})})^2\rangle + 164\langle \delta N_p^{(\mathrm{net})}\delta N_p^{(\mathrm{tot})}\rangle - 75\langle N_p^{(\mathrm{net})}\rangle\right] + O(\alpha^2). \tag{61}$$

Next, let us estimate the value of α in relativistic heavy ion collisions. Under the chemical equilibrium condition, the ratio of the charged pion numbers, $\langle N_{\pi^+}\rangle$ and $\langle N_{\pi^-}\rangle$, having isospin charges ± 1, is given by

$$\frac{\langle N_{\pi^-}\rangle}{\langle N_{\pi^+}\rangle} \simeq e^{-2\mu_{\mathrm{I}}/T}, \tag{62}$$

where we have adopted Boltzmann statistics for pions, since the effect of Bose-Einstein correlation on the pion density is about 10% for $T_{\mathrm{chem}} = m_\pi$ and does not affect our qualitative conclusion. The experimental result for $\langle N_{\pi^-}\rangle/\langle N_{\pi^+}\rangle$ in the final state is almost unity for high-energy collisions in accordance with the approximate isospin symmetry. Substituting Eq. (62) in Eq. (57) and using $\langle N_{\pi^-}\rangle/\langle N_{\pi^+}\rangle - 1 \ll 1$, one

obtains

$$\alpha \simeq \frac{1}{8}\left(\frac{\langle N_{\pi^-}\rangle}{\langle N_{\pi^+}\rangle} - 1\right). \tag{63}$$

The value of α, as well as $\langle N_{\pi^-}\rangle/\langle N_{\pi^+}\rangle - 1$, grows as $\sqrt{s_{\rm NN}}$ is lowered. In order to see how these parameters become non-negligible for small $\sqrt{s_{\rm NN}}$, we focus on the 40-GeV collision at the Super Proton Synchrotron (SPS) ($\sqrt{s_{\rm NN}} \simeq 9$ GeV). For this collision, the experimental value of $\langle N_{\pi^-}\rangle/\langle N_{\pi^+}\rangle$ is 1.05 ± 0.05 [29]. Substituting the worst value within 1σ, $\langle N_{\pi^-}\rangle/\langle N_{\pi^+}\rangle = 1.1$, in Eq. (63), one obtains $\alpha \simeq 1/80$. On the other hand, below the top SPS energy the production of antinucleons is well suppressed and one can replace all $\delta N_p^{\rm (net)}$ and $\delta N_p^{\rm (tot)}$ in Eqs. (58)–(61) with δN_p to a good approximation. Equation (61), for example, then becomes

$$\begin{aligned}\left\langle\left(\delta N_{\rm B}^{\rm (net)}\right)^4\right\rangle_c \simeq{}& 16(1+8\alpha)\langle(\delta N_p)^4\rangle_c - 48(1+10\alpha)\langle(\delta N_p)^3\rangle \\ &+ 60(1+10.1\alpha)\langle(\delta N_p)^2\rangle - 26(1+11.5\alpha)\langle N_p\rangle.\end{aligned} \tag{64}$$

This result shows that for $\alpha = 1/80$ the corrections of nonzero isospin density to Eqs. (50)–(53) are less than 10% in magnitude. The effect is smaller in relations for the lower order cumulants, Eqs. (58)–(60), and formulas for proton number cumulants, Eqs. (46)–(49).

With these results, one can conclude that the formulas for the isospin symmetric case, Eqs. (50)–(53), can safely be used for the analysis of the baryon number cumulants for $\sqrt{s_{\rm NN}} \simeq 9$ GeV with a precision of better than 10%. Because the production of isospin charged particles increases as $\sqrt{s_{\rm NN}}$ goes up, the value of α and hence the effect of nonzero isospin density on Eqs. (50)–(53) are more suppressed for higher energy collisions.

As $\sqrt{s_{\rm NN}}$ is lowered, the value of α grows and eventually approaches the one in the colliding heavy nuclei, $\alpha_A \simeq 0.1$. For $\alpha \simeq 0.1$, the first-order correction in Eq. (64) is comparable with the zeroth-order one. Relations for the isospin symmetric case, Eqs. (50)–(53), therefore, are no longer applicable. For such collision energies, however, conditions required for the factorization given by Eq. (2) themselves break down, as discussed in Sec. II B.

Before closing this section, we recapitulate that the suppression of the isospin density in the nucleon sector, and hence α, in the final state is caused by the production of the large number of particles having isospin charges, especially charged pions. In Appendix B, we present an analysis for this effect.

IV. DISCUSSION

A. Recent experimental results on proton number cumulants

As emphasized in the previous sections, the cumulants of the proton and baryon numbers are in general different. One, therefore, has to be careful when comparing theoretical predictions on baryon number cumulants with experimental proton number ones. In this section, we show that the deviation from the thermal distribution in baryon number cumulants becomes difficult to measure in proton number cumulants using relations obtained in the previous section with some additional assumptions.

In general, it is possible that, while the net baryon number fluctuations in the final state have a considerable deviation from the grand canonical ones reflecting the hysteresis of fireballs and/or global charge conservation, baryon and antibaryon numbers separately follow thermal (Boltzmann) distributions. For example, if the net baryon number fluctuations above $T_{\rm c}$ survive until the final state, the net baryon number fluctuations remain small compared to the thermal ones in the hadronic medium, while baryon and antibaryon number fluctuations separately follow the thermal one. Generally, cumulants of net numbers cannot take arbitrary values; for instance, the second-order cumulant is constrained by the Cauchy-Schwartz inequality:

$$\begin{aligned}&(\sqrt{\langle(\delta N_{\rm B})^2\rangle} - \sqrt{\langle(\delta N_{\bar{\rm B}})^2\rangle})^2 \\ &\quad\leqslant \left\langle\left(\delta N_{\rm B}^{\rm (net)}\right)^2\right\rangle \leqslant (\sqrt{\langle(\delta N_{\rm B})^2\rangle} + \sqrt{\langle(\delta N_{\bar{\rm B}})^2\rangle})^2.\end{aligned} \tag{65}$$

The values of net baryon number cumulants satisfying these constraints are not forbidden. Suppose that, as an extreme case, the net baryon number fluctuations completely vanish and the left equality in Eq. (65) is realized. A baryon and antibaryon distribution function

$$\mathcal{F}(N_{\rm B}, N_{\bar{\rm B}}) = P_\lambda(N_{\rm B})\delta_{N_{\rm B},N_{\bar{\rm B}}}, \tag{66}$$

which is a constrained baryon and antibaryon number distribution following the canonical distribution, constitutes such an example. The distribution function $\mathcal{F}(N_{\rm B}, N_{\bar{\rm B}})$ for a free gas in the grand canonical ensemble, i.e., an unconstrained case, on the other hand, is given by Eq. (8).

Now, let us consider the difference between the net baryon and net proton number cumulants when the baryon and antibaryon number distributions follow Boltzmann statistics while the net baryon number does not. Because of the Boltzmann nature of $N_{\rm B}$ and $N_{\bar{\rm B}}$, distributions of N_p and $N_{\bar{p}}$ are also Poissonian from Eq. (2). Thus, cumulants of the baryon and proton numbers satisfy

$$\begin{aligned}\langle N_{\rm B}\rangle &= \langle(\delta N_{\rm B})^2\rangle = \langle(\delta N_{\rm B})^3\rangle = 2\langle N_p\rangle_{\rm HG} \\ &= 2\langle(\delta N_p)^2\rangle_{\rm HG} = 2\langle(\delta N_p)^3\rangle_{\rm HG} = 2\langle(\delta N_p)^4\rangle_{c,{\rm HG}},\end{aligned} \tag{67}$$

and the same for the antibaryon and antiproton numbers, where $\langle\cdot\rangle_{\rm HG}$ is the expectation value for free hadron gas (HG) composed of mesons and nucleons at $T_{\rm chem}$, i.e., a simplified version of the hadron resonance gas (HRG) model [33]. The factors of 2 in front of the proton number cumulants in Eq. (67) are understood from Eq. (6).

By using Eq. (67), the second terms in Eqs. (47) and (48) are transformed as

$$\begin{aligned}\left\langle N_{\rm B}^{\rm (tot)}\right\rangle &= 2\langle(\delta N_p)^2 + (\delta N_{\bar{p}})^2\rangle_{\rm HG} \\ &= 2\left\langle\left(\delta N_p^{\rm (net)}\right)^2\right\rangle_{\rm HG},\end{aligned} \tag{68}$$

$$\begin{aligned}\left\langle\delta N_{\rm B}^{\rm (net)}\delta N_{\rm B}^{\rm (tot)}\right\rangle &= \langle(\delta N_{\rm B})^2 - (\delta N_{\bar{\rm B}})^2\rangle \\ &= 2\langle(\delta N_p)^3 - (\delta N_{\bar{p}})^3\rangle_{\rm HG} = 2\left\langle\left(\delta N_p^{\rm (net)}\right)^3\right\rangle_{\rm HG},\end{aligned} \tag{69}$$

where in the last equalities we have used the fact that the proton and antiproton numbers do not have correlations in the free gas,

i.e., $\langle \delta N_p \delta N_{\bar{p}} \rangle_{\rm HG} = \langle (\delta N_p)^2 \delta N_{\bar{p}} \rangle_{\rm HG} = \langle \delta N_p (\delta N_{\bar{p}})^2 \rangle_{\rm HG} = 0$. Substituting Eqs. (68) and (69) in Eqs. (47) and (48), respectively, one obtains

$$\left\langle \left(\delta N_p^{(\rm net)}\right)^2 \right\rangle = \tfrac{1}{4} \left\langle \left(\delta N_{\rm B}^{(\rm net)}\right)^2 \right\rangle + \tfrac{1}{2} \left\langle \left(\delta N_p^{(\rm net)}\right)^2 \right\rangle_{\rm HG}, \quad (70)$$

$$\left\langle \left(\delta N_p^{(\rm net)}\right)^3 \right\rangle = \tfrac{1}{8} \left\langle \left(\delta N_{\rm B}^{(\rm net)}\right)^3 \right\rangle + \tfrac{3}{4} \left\langle \left(\delta N_p^{(\rm net)}\right)^3 \right\rangle_{\rm HG}. \quad (71)$$

These results show that the second terms on the RHSs, which come from the binomial distributions of the nucleon isospin, have significant contribution to the cumulants of the proton number, and the contributions of the net baryon number cumulants, $\langle (\delta N_{\rm B}^{(\rm net)})^n \rangle$, are relatively suppressed. Since the second terms give the thermal fluctuations, these results show that the deviation of $\langle (\delta N_{\rm B}^{(\rm net)})^n \rangle$ from the thermal value is hard to see in the proton number cumulants. Although one cannot transform the fourth-order relation Eq. (49) to a simple form as in Eqs. (70) and (71), from the factor of $1/16$ in front of $\langle (\delta N_B^{(\rm net)})^4 \rangle_c$ in Eq. (49) it is obvious that the direct contribution of this term to experimentally measured $\langle (\delta N_p^{(\rm net)})^4 \rangle_c$ is more suppressed compared to the lower order cumulants and that its experimental confirmation is more difficult. These analyses strongly indicate that, even if the baryon number cumulants have considerable deviation from the thermal values, they are obscured in the experimentally measured proton number cumulants due to the redistribution in isospin space. Such a tendency seems to become more prominent for higher order cumulants. It is known that higher order cumulants of the baryon number have large critical exponents and thus can be significantly enhanced in the vicinity of the critical point [10]. The above result, however, indicates that such enhancement is suppressed by a factor of $1/2^n$ and difficult to measure in experiments in proton number cumulants. The analysis of the baryon number cumulants with Eqs. (50)–(53) enables us to remove the thermal contribution in the proton number cumulants and makes the direct experimental observation of signals in $\langle (\delta N_p^{(\rm net)})^n \rangle_c$ possible.

The $\sqrt{s_{\rm NN}}$ dependencies of proton number cumulants have recently been measured by the STAR Collaboration at the RHIC [4,5]. The experimental result shows that ratios between net proton number cumulants follow the prediction of the HRG model within about 10% precision. We, however, emphasize that one should not conclude from this result that baryon number cumulants also follow the prediction of the HRG model within 10% precision. As demonstrated above, the binomial nature of the isospin distribution makes proton number cumulants close to the ones in the HRG model. In this sense, it is interesting that the experimental results for skewness and kurtosis nevertheless have small but significant deviations from the HRG predictions [5]. The deviation, for example, in skewness, can be a consequence of $\langle (\delta N_{\rm B}^{(\rm net)})^3 \rangle$ in Eq. (71), which possibly reflects the properties of the matter in the early stage.

A remark on Eqs. (70) and (71) is in order. These formulas are obtained with the assumption that baryon and antibaryon number distributions are Poissonian, while the net baryon number is not. When one further assumes that the net baryon number cumulants also follow the thermal distribution in these results, these formulas simply reproduce the free gas result

$$\left\langle \left(\delta N_{\rm B}^{(\rm net)}\right)^n \right\rangle_c = 2 \left\langle \left(\delta N_p^{(\rm net)}\right)^n \right\rangle_{c,\rm HG} \quad (72)$$

as they should do. This is easily checked by substituting $\langle (\delta N_p^{(\rm net)})^n \rangle = \langle (\delta N_p^{(\rm net)})^n \rangle_{\rm HG}$ in Eqs. (70) and (71).

In this section, we considered the experimental results on proton number cumulants using the results in Sec. III. More direct application of these formulas, i.e., to determine baryon number cumulants from experimental results on proton number cumulants with Eqs. (50)–(53), remains to be done. The baryon number cumulants obtained in this way are to be compared with various theoretical predictions.

B. Efficiency and acceptance corrections

So far, we have considered the reconstruction of the missing information for the neutron number in experiments using Eq. (2). It is possible to extend this argument to infer different information from the event-by-event analysis.

An example is the evaluation of the effect of efficiency and acceptance of detectors. The experimental detectors usually do not have 2π acceptance. Moreover, protons entering a detector are identified with some efficiency. If one can assume that protons (antiprotons) in the final state are detected by the detector with a fixed probability σ ($\bar{\sigma}$) independent of momentum, multiplicity, and so on, and the efficiency for each particle does not have correlations, the distribution function $\mathcal{G}^{(\rm obs)}(N_p^{(\rm obs)}, N_{\bar{p}}^{(\rm obs)})$ for the observed proton and antiproton numbers, $N_p^{(\rm obs)}$ and $N_{\bar{p}}^{(\rm obs)}$, respectively, are related to the one for all particles entering the detector, N_p and $N_{\bar{p}}$, as

$$\mathcal{G}^{(\rm obs)}\left(N_p^{(\rm obs)}, N_{\bar{p}}^{(\rm obs)}\right) = \sum_{N_p, N_{\bar{p}}} \mathcal{G}(N_p, N_{\bar{p}}) B_\sigma\left(N_p^{(\rm obs)}; N_p\right) B_{\bar{\sigma}}\left(N_{\bar{p}}^{(\rm obs)}; N_{\bar{p}}\right), \quad (73)$$

or substituting Eq. (16) in this result and using the property of the binomial distribution one obtains

$$\mathcal{G}^{(\rm obs)}\left(N_p^{(\rm obs)}, N_{\bar{p}}^{(\rm obs)}\right) = \sum_{N_B, N_{\bar{B}}} \mathcal{F}(N_{\rm B}, N_{\bar{\rm B}}) B_{r\sigma}\left(N_p^{(\rm obs)}; N_B\right) B_{\bar{r}\bar{\sigma}}\left(N_{\bar{p}}^{(\rm obs)}; N_{\bar{B}}\right). \quad (74)$$

Equation (74) indicates that when the deviations of σ and $\bar{\sigma}$ from unity become large, they affect cumulants with different orders differently. The effect of efficiency, therefore, cannot be canceled out by taking the ratio between cumulants. In particular, as σ and $\bar{\sigma}$ become smaller, $\mathcal{G}^{(\rm obs)}(N_p^{(\rm obs)}, N_{\bar{p}}^{(\rm obs)})$ approach the product of independent Poisson distributions irrespective of the form of $\mathcal{F}(N_{\rm B}, N_{\bar{\rm B}})$. This would be another reason for the present experimental results on proton number cumulants [5], which is consistent with the HRG model.

Other experimental artifacts which have not been taken into account yet in experimental analyses are background and misidentified protons. In particular, according to Ref. [34], the contamination from knockout protons is not negligible. By their nature, they give a Poissonian contribution and make the observed proton number cumulants approach the Poissonian

values. Indeed, the HIJING + GEANT simulation in Ref. [4] shows that these effects are considerable.

V. SUMMARY

The most important results of the present paper are summarized in Eqs. (46)–(49) and Eqs. (50)–(53), which are formulas relating baryon and proton number cumulants in the final state in heavy ion collisions. The baryon number cumulants are a conserved charge and one of the fluctuation observables which is most widely analyzed in theoretical studies. Our results enable us to determine the baryon number cumulants with experimental results in heavy ion collisions, and hence they make the direct comparison between theoretical predictions and experiments possible. Such a comparison will provide significant information on the QCD phase diagram. Equations (46)–(53) are obtained on the basis of the binomial nature of the nucleon and antinucleon number distributions in isospin space, which is justified for $\sqrt{s_{\rm NN}} \gtrsim 10$ GeV. Although these results are obtained for an isospin-symmetric medium, the effect of nonzero isospin density in relativistic heavy ion collisions is well suppressed in this energy range because of the abundance of the created pions.

ACKNOWLEDGMENTS

The authors are grateful for stimulating discussions at the workshop "Fluctuations, Correlations and RHIC Low Energy Runs" held at the Brookhaven National Laboratory, USA, October 3–5, 2011. This work is supported in part by Grants-in-Aid for Scientific Research by Monbu-Kagakusyo of Japan (No. 21740182 and No. 23540307).

APPENDIX A: BARYON AND PROTON NUMBER CUMULANTS

In this Appendix, we derive Eqs. (37)–(44). To obtain these relations, we start from the cumulant-generating function Eq. (31),

$$K(\theta,\bar\theta) = \log \sum_F \exp[k(\theta,\bar\theta)], \tag{A1}$$

where $\sum_F$ is a shorthand notation for $\sum_{N_{\rm B},N_{\bar{\rm B}}} \mathcal{F}(N_{\rm B},N_{\bar{\rm B}})$. In this Appendix, we also suppress the subscript in $k_{N_{\rm B},N_{\bar{\rm B}}}(\theta,\bar\theta)$.

We require the following four conditions for the properties of $k(\theta,\bar\theta)$:

$$k(0,0) = 0, \tag{A2}$$

$$\frac{\partial^n}{\partial\theta^n} k(0,0) = \xi_n N_{\rm B}, \tag{A3}$$

$$\frac{\partial^n}{\partial\bar\theta^n} k(0,0) = \bar\xi_n N_{\bar{\rm B}}, \tag{A4}$$

$$\frac{\partial^{n+m}}{\partial\theta^n\partial\bar\theta^m} k(0,0) = 0, \tag{A5}$$

for positive integers n and m. Eq. (A2) is satisfied for probability distribution functions normalized to unity. Equations (A3)–(A5) are Eqs. (33)–(35) in the text. All calculations in this Appendix are based only on these constraints on $K(\theta,\bar\theta)$.

1. Net proton number cumulants

By using $K(\theta,\bar\theta)$, the net proton number cumulants are given by

$$\left\langle \left(\delta N_p^{(\rm net)}\right)^n \right\rangle_c = \left(\frac{\partial}{\partial\theta} - \frac{\partial}{\partial\bar\theta}\right)^n K(0,0). \tag{A6}$$

To proceed to calculate Eq. (A6), it is convenient to use the cumulant expansion of Eq. (A1),

$$\begin{aligned} K(\theta,\bar\theta) &= \sum_m \frac{1}{m!} \sum_F [k(\theta,\bar\theta)]_c^m \\ &= 1 + \sum_F k(\theta,\bar\theta) + \frac{1}{2}\sum_F [\delta k(\theta,\bar\theta)]^2 \\ &\quad + \frac{1}{3!}\sum_F [\delta k(\theta,\bar\theta)]^3 + \frac{1}{4!}\sum_F [\delta k(\theta,\bar\theta)]_c^4 + \cdots . \end{aligned} \tag{A7}$$

Each term on the far right-hand side defines each cumulant, $\sum_F [k(\theta,\bar\theta)]_c^m$, up to the fourth order, with

$$\delta k(\theta,\bar\theta) = k(\theta,\bar\theta) - \sum_F k(\theta,\bar\theta), \tag{A8}$$

$$\sum_F [\delta k(\theta,\bar\theta)]_c^4 = \sum_F [\delta k(\theta,\bar\theta)]^4 - 3\left(\sum_F [\delta k(\theta,\bar\theta)]^2\right)^2. \tag{A9}$$

Because of Eq. (A2), all $k(\theta,\bar\theta)$ and $\delta k(\theta,\bar\theta)$ in the term in Eq. (A7) must receive at least one differentiation so that the term gives a nonzero contribution to Eq. (A6). This immediately means that the mth-order term in Eq. (A7) can affect Eq. (A6) only if $m \leqslant n$.

The first-order net proton number cumulant, Eq. (37), is calculated to be

$$\begin{aligned} \left\langle N_p^{(\rm net)} \right\rangle &= (\partial_\theta - \partial_{\bar\theta}) K(0,0) = \sum_F (\partial_\theta - \partial_{\bar\theta}) k(0,0) \\ &= \sum_F (\xi_1 N_{\rm B} - \bar\xi_1 N_{\bar{\rm B}}) = \langle \xi_1 N_{\rm B} - \bar\xi_1 N_{\bar{\rm B}} \rangle, \end{aligned} \tag{A10}$$

with $\partial_\theta \equiv \partial/\partial\theta$ and $\partial_{\bar\theta} \equiv \partial/\partial\bar\theta$. In the third equality in Eq. (A10), we have used Eqs. (A3) and (A4). The second-order relation, Eq. (38), is obtained as follows:

$$\begin{aligned} &\left\langle \left(\delta N_p^{(\rm net)}\right)^2 \right\rangle \\ &= (\partial_\theta - \partial_{\bar\theta})^2 K(0,0) \\ &= \sum_F (\partial_\theta - \partial_{\bar\theta})^2 k(0,0) + \frac{1}{2}\sum_F (\partial_\theta - \partial_{\bar\theta})^2 [\delta k(0,0)]^2 \\ &= \sum_F (\partial_\theta^2 + \partial_{\bar\theta}^2) k(0,0) + 2\times\frac{1}{2}\sum_F [(\partial_\theta - \partial_{\bar\theta})\delta k(0,0)]^2 \\ &= \xi_2 \langle N_{\rm B}\rangle + \bar\xi_2 \langle N_{\bar{\rm B}}\rangle + \langle (\xi_1 \delta N_{\rm B} - \bar\xi_1 \delta N_{\bar{\rm B}})^2 \rangle. \end{aligned} \tag{A11}$$

To obtain the third line, we have used Eqs. (A5) and (A2) for the first and second terms, respectively. The factor of 2 in the second term comes from the number of outcomes of the application of the two derivatives to the two $\delta k(\theta, \bar{\theta})$ in the second line. Equations (A3) and (A4) are used in the last equality.

Similar manipulations lead to Eqs. (39) and (40). We note that the relation

$$(\partial_\theta - \partial_{\bar{\theta}})^4 \sum_F [\delta k(\theta, \bar{\theta})]_c^4 = 4! \sum_F [(\partial_\theta - \partial_{\bar{\theta}}) k(\theta, \bar{\theta})]_c^4 \quad \text{(A12)}$$

makes the calculation for the fourth-order cumulant more concise.

2. Net baryon number cumulants

To obtain Eqs. (41)–(44), we start from the following relation for the net baryon number cumulants:

$$\left\langle \left(\delta N_{\rm B}^{(\rm net)}\right)^n \right\rangle_c = \sum_F \left[\left(\xi_1^{-1}\partial_\theta - \bar{\xi}_1^{-1}\partial_{\bar{\theta}}\right) k \right]_c^n \equiv \sum_F [\partial_\xi k]_c^n, \quad \text{(A13)}$$

with $\partial_\xi = \xi_1^{-1}\partial_\theta - \bar{\xi}_1^{-1}\partial_{\bar{\theta}}$. We suppress arguments in $K(0, 0)$ and $k(0, 0)$ throughout this section.

The manipulation of Eq. (A13) for $n = 1$ is trivial. For $n = 2$, Eq. (A13) is calculated to be

$$\begin{aligned} \left\langle \left(\delta N_{\rm B}^{(\rm net)}\right)^2 \right\rangle &= \sum_F (\partial_\xi \delta k)^2 = \frac{1}{2}\partial_\xi^2 \sum_F (\delta k)^2 \\ &= \partial_\xi^2 K - \sum_F \partial_\xi^2 k = \partial_{(1)}^2 K - \partial_{(2)} K \\ &= \left\langle \left(\frac{\delta N_p}{\xi_1} - \frac{\delta N_{\bar{p}}}{\bar{\xi}_1} \right)^2 \right\rangle - \left\langle \frac{\xi_2}{\xi_1^3} N_p + \frac{\bar{\xi}_2}{\bar{\xi}_1^3} N_{\bar{p}} \right\rangle. \quad \text{(A14)} \end{aligned}$$

In the second line, we introduced the symbol

$$\partial_{(n)} = \frac{\xi_n}{\xi_1^{n+1}}\partial_\theta + (-1)^n \frac{\bar{\xi}_n}{\bar{\xi}_1^{n+1}}\partial_{\bar{\theta}} \quad \text{(A15)}$$

and used the relation

$$\begin{aligned} \partial_\xi^n k &= \left(\frac{1}{\xi_1^n}\partial_\theta^n + \frac{1}{\bar{\xi}_1^n}\partial_{\bar{\theta}}^n \right) k \\ &= \left(\frac{\xi_n}{\xi_1^{n+1}}\partial_\theta + (-1)^n \frac{\bar{\xi}_n}{\bar{\xi}_1^{n+1}}\partial_{\bar{\theta}} \right) k = \partial_{(n)} k, \quad \text{(A16)} \end{aligned}$$

where we have used Eqs. (A3)–(A5). The last equality in Eq. (A14) comes from the definition of K.

To proceed to $n \geqslant 3$, we first introduce the following notation:

$$\partial_{(n,m)} = \frac{\xi_n \xi_m}{\xi_1^{n+m+1}}\partial_\theta + (-1)^{n+m+1}(* \to \bar{*}), \quad \text{(A17)}$$

$$\partial_{(n,m,l)} = \frac{\xi_n \xi_m \xi_l}{\xi_1^{n+m+l+1}}\partial_\theta + (-1)^{n+m+l+2}(* \to \bar{*}), \quad \text{(A18)}$$

for positive integers n, m, and l. $\partial_{(n_1,n_2,\cdots,n_i)}$ for $i > 3$ is also defined as in Eqs. (A15), (A17), and (A18). One easily finds that (i) $\partial_{(n,m,\cdots,l)}$ are invariant under the permutations of the subscripts, for example, $\partial_{(n,m,l)} = \partial_{(m,n,l)}$, and (ii) when a subscript is one, it can be eliminated, e.g., $\partial_{(n,m,1)} = \partial_{(n,m)}$, while $\partial_{(1)} = \partial_\xi$. With this notation, the derivatives of δk are written as

$$\partial_\xi^n \delta k = \partial_{(n)} \delta k, \quad \text{(A19)}$$

$$\partial_{(n)}\partial_{(m)} \delta k = \partial_{(n,m,2)} \delta k, \quad \text{(A20)}$$

$$\partial_{(n)}\partial_{(m)}\partial_{(l)} \delta k = \partial_{(n,m,l,3)} \delta k, \quad \text{(A21)}$$

and so forth.

By using these relations, for example, Eq. (A13) for $n = 3$ is calculated as

$$\begin{aligned} \left\langle \left(\delta N_{\rm B}^{(\rm net)}\right)^3 \right\rangle &= \sum_F (\partial_\xi \delta k)^3 \\ &= \partial_\xi^3 K - 3\sum_F \left(\partial_\xi^2 \delta k\right)(\partial_\xi \delta k) - \sum_F \partial_\xi^3 k \\ &= \partial_{(1)}^3 K - 3\sum_F (\partial_{(2)}\delta k)(\partial_{(1)}\delta k) - \sum_F \partial_{(3)} k \\ &= \partial_{(1)}^3 K - 3(\partial_{(2)}\partial_{(1)} K - \partial_{(2,2)} K) - \partial_{(3)} K, \quad \text{(A22)} \end{aligned}$$

which leads to Eq. (43). In the second and last equalities, we used

$$\partial_\xi^3 K = \sum_F (\partial_\xi \delta k)^3 + 3\sum_F \left(\partial_\xi^2 \delta k\right)(\partial_\xi \delta k) + \sum_F \partial_\xi^3 k, \quad \text{(A23)}$$

$$\partial_{(n)}\partial_{(m)} K = \partial_{(n,m,2)} K + \sum_F (\partial_{(n)}\delta k)(\partial_{(m)}\delta k). \quad \text{(A24)}$$

A similar manipulation for $n = 4$ leads to

$$\begin{aligned} \left\langle \left(\delta N_{\rm B}^{(\rm net)}\right)^4 \right\rangle_c &= \partial_{(1)}^4 K - 6\partial_{(2)}\partial_{(1)}^2 K + 12\partial_{(2,2)}\partial_{(1)} K \\ &\quad + 3\partial_{(2)}^2 K - 4\partial_{(3)}\partial_{(1)} K - 15\partial_{(2,2,2)} K \\ &\quad + 10\partial_{(2,3)} K - \partial_{(4)} K, \quad \text{(A25)} \end{aligned}$$

which gives Eq. (44).

APPENDIX B: ISOSPIN DENSITY IN THE FINAL STATE

In this Appendix, we demonstrate that the isospin density of nucleons in the final state of heavy ion collisions is suppressed owing to the abundant production of particles having nonzero isospin charges.

To simplify the calculation, we consider a gas composed of nucleons and pions in chemical equilibrium, and we assume that pions and (anti)nucleons obey Boltzmann statistics, since this approximation does not alter the qualitative conclusion in this Appendix. Under these assumptions, the ratios between the numbers of (anti)protons and (anti)neutrons in a phase space are given in terms of $\mu_{\rm I}$ and T as

$$\frac{N_p}{N_n} = \frac{N_{\bar{n}}}{N_{\bar{p}}} = e^{\mu_{\rm I}/T} = \frac{1-2\alpha}{1+2\alpha}, \quad \text{(B1)}$$

with $\alpha = N_p/(N_p + N_n)$, and the ratio of the numbers of π^+ and π^- is given by

$$\frac{N_{\pi^+}}{N_{\pi^-}} = e^{2\mu_{\rm I}/T}. \quad \text{(B2)}$$

With these relations, the total isospin in the phase space is calculated to be

$$N_{\rm I} = \frac{1}{2}(N_p - N_n - N_{\bar{p}} + N_{\bar{n}}) + N_{\pi^+} - N_{\pi^-} = \alpha\left(N_{\rm N} + N_{\bar{\rm N}} + \frac{4}{1-4\alpha^2}N_{\pi_{\rm ch}}\right), \tag{B3}$$

with the number of charged pions $N_{\pi_{\rm ch}} = N_{\pi^+} + N_{\pi^-}$.

In the initial state of heavy ion collisions, the isospin asymmetry of the colliding heavy nuclei α_A is $(N_n - N_p)/[2(N_p + N_n)] \simeq 0.1$. Assuming that this isospin asymmetry equally distributes along the rapidity direction in the final state, one has $N_{\rm I}/N_{\rm N}^{\rm (net)} \simeq \alpha_A$. With Eq. (B3), one then obtains

$$\alpha\left(\frac{N_N^{\rm (tot)}}{N_N^{\rm (net)}} + \frac{4}{1-4\alpha^2}\frac{N_{\pi_{\rm ch}}}{N_N^{\rm (net)}}\right) \simeq \alpha_A. \tag{B4}$$

The term in the parentheses is larger than unity, and it becomes larger as more charged pions and antinucleons are produced. Equation (B4) thus shows that the value of α is more suppressed than α_A owing to the production of these particles. If the contribution of other particles with nonzero isospin charges is taken into account, the value of α is further suppressed.

[1] I. Arsene *et al.* (BRAHMS Collaboration), Nucl. Phys. A **757**, 1 (2005); B. B. Back *et al.* (PHOBOS Collaboration), *ibid.* **757**, 28 (2005); J. Adams *et al.* (STAR Collaboration), *ibid.* **757**, 102 (2005); K. Adcox *et al.* (PHENIX Collaboration), *ibid.* **757**, 184 (2005).

[2] M. Asakawa and K. Yazaki, Nucl. Phys. A **504**, 668 (1989).

[3] M. A. Stephanov, PoS **LAT2006**, 024 (2006).

[4] M. M. Aggarwal *et al.* (STAR Collaboration), Phys. Rev. Lett. **105**, 022302 (2010).

[5] B. Mohanty (STAR Collaboration), J. Phys. G **38**, 124023 (2011); S. Kabana (STAR Collaboration), arXiv:1203.1814 [nucl-ex].

[6] M. Bleicher, J. Phys. G **38**, 124035 (2011).

[7] V. Koch, arXiv:0810.2520 [nucl-th].

[8] M. A. Stephanov, K. Rajagopal, and E. V. Shuryak, Phys. Rev. Lett. **81**, 4816 (1998); Phys. Rev. D **60**, 114028 (1999).

[9] Y. Hatta and M. A. Stephanov, Phys. Rev. Lett. **91**, 102003 (2003); **91**, 129901 (2003).

[10] M. A. Stephanov, Phys. Rev. Lett. **102**, 032301 (2009).

[11] C. Athanasiou, K. Rajagopal, and M. Stephanov, Phys. Rev. D **82**, 074008 (2010).

[12] E. S. Fraga, L. F. Palhares, and P. Sorensen, Phys. Rev. C **84**, 011903 (2011).

[13] M. Asakawa, U. W. Heinz, and B. Müller, Phys. Rev. Lett. **85**, 2072 (2000).

[14] S. Jeon and V. Koch, Phys. Rev. Lett. **85**, 2076 (2000).

[15] V. Koch, A. Majumder, and J. Randrup, Phys. Rev. Lett. **95**, 182301 (2005).

[16] S. Ejiri, F. Karsch, and K. Redlich, Phys. Lett. B **633**, 275 (2006).

[17] M. Asakawa, S. Ejiri, and M. Kitazawa, Phys. Rev. Lett. **103**, 262301 (2009).

[18] B. Friman *et al.*, Eur. Phys. J. C **71**, 1694 (2011).

[19] M. A. Stephanov, Phys. Rev. Lett. **107**, 052301 (2011).

[20] R. V. Gavai and S. Gupta, Phys. Lett. B **696**, 459 (2011)].

[21] C. Schmidt, Prog. Theor. Phys. Suppl. **186**, 563 (2010)].

[22] S. Mukherjee, J. Phys. G **38**, 124022 (2011).

[23] S. Borsanyi *et al.*, J. High Energy Phys. 12 (2012) 138.

[24] A. Bazavov *et al.* (HotQCD Collaboration), arXiv:1203.0784 [hep-lat].

[25] M. Kitazawa and M. Asakawa, Phys. Rev. C **85**, 021901(R) (2012).

[26] J. Cleymans and K. Redlich, Phys. Rev. Lett. **81**, 5284 (1998).

[27] The Review of Particle Physics, K. Nakamura *et al.* (Particle Data Group), J. Phys. G **37**, 075021 (2010).

[28] C. Nonaka and S. A. Bass, Phys. Rev. C **75**, 014902 (2007).

[29] P. Braun-Munzinger, K. Redlich, and J. Stachel, in *Quark Gluon Plasma 3*, edited by R. C. Hwa and X.-N. Wang (World Scientific, Singapore, 2003), p. 491.

[30] B. Schenke, S. Jeon, and C. Gale, Phys. Rev. C **82**, 014903 (2010).

[31] Y. Pang, T. J. Schlagel, and S. H. Kahana, Phys. Rev. Lett. **68**, 2743 (1992).

[32] P. Braun-Munzinger, B. Friman, F. Karsch, K. Redlich, and V. Skokov, Phys. Rev. C **84**, 064911 (2011); Nucl. Phys. A **880**, 48 (2012).

[33] F. Karsch and K. Redlich, Phys. Lett. B **695**, 136 (2011).

[34] B. I. Abelev *et al.* (STAR Collaboration), Phys. Rev. C **79**, 034909 (2009).